Javaid *et al. EURASIP Journal on Wireless Communications and Networking* (2016) 2016:147
DOI 10.1186/s13638-016-0643-z

EURASIP Journal on Wireless Communications and Networking

RESEARCH Open Access

# Modeling induction and routing to monitor hospitalized patients in multi-hop mobility-aware body area sensor networks

Nadeem Javaid[1*], Ashfaq Ahmad[1], Anum Tauqir[2], Muhammad Imran[3], Mohsen Guizani[4], Zahoor Ali Khan[5] and Umar Qasim[6]

**Abstract**

In wireless body area sensor networks (WBASNs), energy efficiency is an area of extreme significance. At first, we present a mathematical model for a non-invasive inductive link which is used to recharge the battery of an implanted biomedical device (pacemaker). Afterwards, we propose a distance-aware relaying energy-efficient (DARE) and mutual information-based DARE (MI-DARE) routing protocols for multihop mobility-aware body area sensor networks (MM-BASNs). Both the routing protocols and the non-invasive inductive link model are tested with the consideration of eight patients in a hospital unit under different topologies, where the vital signs of each patient are monitored through seven on-body sensors and an implanted pacemaker. To reduce energy consumption of the network, the sensors communicate with a sink via an on-body relay which is fixed on the chest of each patient. The behavior (static/mobile) and position of the sink are changed in each topology, and the impact of mobility due to postural changes of the patient(s) arms, legs, and head is also investigated. The MI-DARE protocol further prolongs the network lifetime by minimizing the number of transmissions. Simulation results show that the proposed techniques outperform contemporary schemes in terms of the selected performance metrics.

**Keywords:** WBASN, Network lifetime, Energy consumption, Mobility, Inductive link, Implant, Link efficiency, Voltage gain

## 1 Introduction

Wireless sensor networks specifically designed for monitoring different parameters of human body is known as WBASNs. These networks are gradually making advancements due to emerging paradigms like machine-to-machine communication, cyber physical systems, etc. [1]. These networks are used to monitor people that are involved in different activities such as sports, astronaut training, and patients in a hospital or home (see Fig. 1). These patient monitoring systems enable the medical personnel to provide urgent medical aid [2] and prevent patients suffering from poor health condition(s): body stiffness, muscular weaknesses, dependency on the nurses to get their postures changed, etc.

The sensors are equipped with limited energy resources. A major portion of their energy is used to gather data about body organs and transmit it to the end station [3–6]. During this process, some energy is also dissipated in the form of heat. Keeping this issue in mind, research is still underway to reduce the energy consumption of sensors and to prolong the lifetime of the network. In order to keep the nodes alive for a longer period of time, there are many ways/techniques, including energy-efficient routing protocols, inductive models to prolong the batteries of the implanted devices [7], network coding-based cooperative communication [8], local information exchange to handle high traffic between co-located nodes [9], quality of service-aware energy management [10], etc. However, the scope of this research work is only limited to energy-efficient routing protocols and inductive link models.

*Correspondence: nadeemjavaidqau@gmail.com; www.njavaid.com
[1] COMSATS Institute of Information Technology, Islamabad, Pakistan
Full list of author information is available at the end of the article

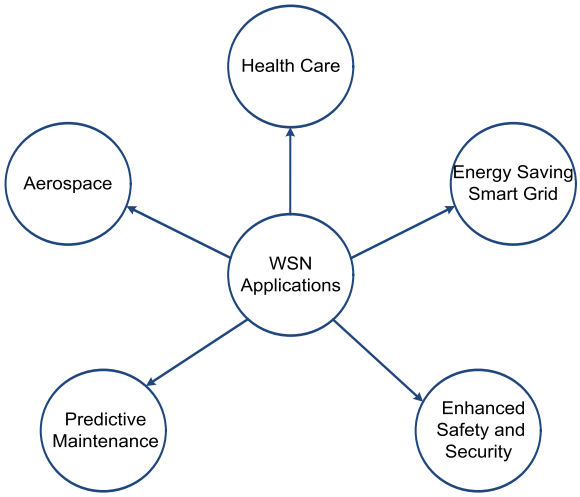


**Fig. 1** WSN applications

In spite of their advantages, WBASNs face many issues, one of these is the limited energy [11] of both the on-body sensors and the in vivo pacemaker. The battery of the sensor/pacemaker exhausts quickly due to continuous communication. When the in vivo pacemaker or the sensor nodes deplete their energy, then it is either almost impossible (infeasible) to replace their batteries. In literature, many routing protocols have been proposed to prolong the battery lifetime of on-body sensors [12–14]. Similarly, many inductive links are designed to maximize the lifetime of pacemaker [15–17]. However, none of these works has jointly considered both problems. Thus, the motivation to enhance the lifetime of on-body sensors leads us to propose DARE and mutual information-based DARE (MI-DARE) routing protocols, and the motivation to recharge the implanted battery of pacemaker leads us to present a mathematical model for the non-invasive inductive link. However, patients under monitoring may show some degree of mobility such as postural changes of on-bed patients that may lead to topological changes and issues such as degradation in link quality and isolation of nodes from the network [18]. The network should be structured in such a way that the nodes are enabled to cater for these issues and provide satisfactory level of communication sessions. In order to account for the mobility, both the routing protocols and the non-invasive inductive link model are tested with the consideration of different topologies (scenarios 1 to 5 illustrated via Figs. 10a, 12, 13, and 14) in a hospital unit. The unit consists of eight properly aligned patients such that each one is equipped with seven on-body sensors, one relay, and an in-body pacemaker. In each scenario, placement of the sensors is kept the same, only the sink node is made mobile or static. Simulation results show that our proposed techniques perform better than the existing mobility-supporting adaptive threshold-based thermal-aware energy-efficient multi-hop protocol (M-ATTEMPT) [19] technique in terms of the selected performance metrics.

It is worth mentioning here that this work is an extended form of our previous works published in [20, 21]. This paper contributes in the following major ways/aspects.

- Our existing work in [21] only considers on-body sensors/relays. Similarly, our work in [20] only considers the implanted pacemaker. In this paper, both works are combined, i.e., the patients are equipped with on-body sensors and an implanted pacemaker. This consideration makes the simulation scenarios (1 to 5) different from our work in [21].
- Unlike [21], the impact of mobility due to postural changes of the patient(s) arms, legs, and head is also considered.
- In this paper, an enhanced version of our previously proposed DARE protocol in [21] is presented, i.e., MI-DARE. The newly proposed MI-DARE protocol uses MI-based machine learning technique to prolong the network lifetime of sensors by minimizing the number of redundant transmissions.
- In this paper, the mathematical model for the non-invasive inductive link includes a fly back diode to prevent voltage surge(s) which was not the case in our previous work in [20]. Moreover, Section 6 related to the mathematical model has been strengthened with the addition of quality factor analysis.

The remainder of this paper is organized as follows. Section 2 overviews the previous research work done on WBASN communications related to patient's mobility, monitoring patients' vital signs, and induction techniques. In Section 3, the system model is presented. Section 4 describes the mathematical model for induction link. Details of the proposed protocols DARE and MI-DARE are explained in Section 5. Section 6 discusses the simulation results. Finally, Section 7 provides the conclusion and future work.

## 2 Related work

The presence of diversified platforms on which the sensor network technology has been built justify that WBASN is a potential research area. Since the last decade, researchers have used sensors to capture real-time vital signs of patients. On the other hand, extensive research has been conducted and is still underway to design efficient inductive links for medical implants. In this section, we summarize previous research attempts with respect to efficient inductive link design and energy-efficient routing protocols.

### 2.1 Inductive link design

In [22], authors present a survey with respect to current development and future demands on implantable and wearable WBASN systems. The authors focus on state-of-the-art technology to provide patients and elders with quality care. Besides discussion on design considerations like energy efficiency, scalability, unobtrusiveness, and security, the authors also discuss benefits and drawbacks of the wearable and implantable WBASN systems. In [15], a generalized voltage-driven model of an inductive link for medical implants is presented. In addition, different parameters are analyzed with respect to resonating impedances. The series resonating impedances improve in voltage gain, while not causing the link efficiency to alter. In [16], an inductive power system is presented which combines power transfer with data transmission for implantable microdevices. The implanted devices receive power from an external transmitter through an inductive link between an external power transmission coil and the implanted receiving coil. The authors in [17] design a transcutaneous link for medical implants by using inductively coupled coils. They also describe the design of an indigenously developed transcutaneous link from commercial off-the-shelf components to demonstrate the design process. Moreover, their work provides an outline for inductive coils and optimized parameters of class E amplifiers. Their experimental results show approximately 40 % link efficiency at 2.5-MHz operating frequency and an output power of 100 mW. In [23], a medical relevance of the monitoring of deformation of implants is presented. It is a powerful tool to evaluate nursing and rehabilitation exercises for tracing dangerous overloads while anticipating implant failure and observing the healing process. The authors also present two implantable wireless designs which are charged via magnetic induction.

### 2.2 Energy-efficient routing

In [13], the authors use relaying and cooperation to prolong the network lifetime. They also investigate path loss while considering different body parts for both single-hop and multi-hop topologies. Similarly, the authors in [24] use topology control to account for access delays due to the underlying medium access control (MAC) layer, however, at the cost of high energy consumption. In [25], the authors set an upper bound to determine the number of relay nodes, sensors, and their respective distances to the sink. Each sensor node performs single-hop communication while relaying nodes perform multi-hop communication to the sink. In [14], J. Elias et al. provide an optimal design for WBASNs by studying the joint data routing and relay positioning problem in order to increase the network lifetime. In this research work, the authors present an inter-based linear programming model which aims for (i) optimized number of relay positions, (ii) minimization of energy consumption of sensors and relays, and (iii) minimization of the installation cost. Simulation results show that this framework has a very short computing time as compared to the other frameworks. In [26], the authors study propagation models subject to network lifetime prolongation. These models reveal that single-hop communication is inefficient for far away nodes from the sink and the multi-hop communication is more suitable. In order to avoid hot spot links, extra nodes in the network, i.e., dedicated relay devices, are introduced. The authors in [19] propose M-ATTEMPT routing protocol in which they use single-hop communication for the delivery critical data and multi-hop communication for the delivery of normal data. In order to prevent damage of body tissues, they also introduce a temperature sensing mechanism to detect the hot spot problem of in-body sensors. In [27], Chen et al. introduce a new interference-aware WBASN that can continuously monitor vital signs of multiple patients and efficiently prioritize data transmission based on patients' conditions. The authors proposed a solution that is based on an integrated hybrid scheduler which guarantees end-to-end delay with the capability to select the best possible route (best link quality) and minimum generated interference which results in high end-to-end packet reliability. In [28], sensing is considered as a service while improving energy efficiency. Thus, the authors present a unique set of design challenges and propose different solutions which are very helpful for current as well as future researchers. In [29], the authors present anycast routing protocol for monitoring patients vital signs while coping with the end-to-end traffic. To achieve minimum network latency, the protocol chooses a nearest data receiver related to the patient. The wireless network performs fall detection, indoor positioning, and electrocardiogram (ECG) monitoring for the patients. Whenever, a fall is detected, the hospital crew gets intimated of the exact position of the patient. In [30], the authors present a cluster-based self-organization protocol. It focuses on relaying data via cluster heads to improve energy efficiency. Initially, the protocol builds a cluster-based structure and then efficiently transmits packets from source to destination. An interesting feature of this technique is the stability in terms of the selected number of cluster heads per round. In [31], the authors balance load of the sensor nodes by presenting a global routing protocol which is tested against real-time experiments along with computer-based simulations. Similarly, [32] introduces a personal wireless hub to collect personal health information of its user(s) through biomedical sensors. The sensed information is securely routed towards the health care unit if found eligible. In [33], Otto et al. present a prototype system for the health monitoring of people/patients at home. The system consists of an uninterrupted WBASN and a home health server. The

WBASN sensors sense heart rate and locomotive activity such that the sensed information is periodically uploaded at the home server. The home server may integrate this information with a local database for user inspection, or it may further be forwarded to a medical server. Similarly, the idea of embedding medical devices with hospital information system is presented in [34]. The integration of ubiquitous echograph with the home information network make it very easy for the doctors to immediately diagnose the patients. In [35], Wang et al. present a distributed WBASN model for medical supervision. The system consists of three tiers: sensor network tier, mobile computing network tier, and remote monitoring network tier. This model provides collection, demonstration, and storage of vital information like ECG, blood oxygen, body temperature, and respiration rate. The system demonstrates many advantages such as low-power, easy configuration, convenient carrying, and real-time reliable data. In [36], the authors use wearable sensors to monitor daily activities of humans which they perform during different activities. The correct monitoring of these complex actions is challenging. For this purpose, they introduce activity recognition with the help of wearable sensing devices.

## 3 System model

The system under consideration is a hospital ward with dimensions of 12 m $\times$ 6 m, under five different scenarios (discussed in simulation section) in which the patients are monitored to detect any ambiguity in the normal functioning. The following subsections discuss in detail the system specifications, the network topology, the types of data reporting, functionality of the pacemaker, and the induction link along with its parameters.

### 3.1 Network topology

Each patient is equipped with seven on-body sensors, a body relay (BR), and an in-body pacemaker as shown in Fig. 2. This topology is kept the same for all the patients in the entire ward such that the total number of sensors are 56 body sensors, 8 body relays, and a pacemaker. All these sensors are equipped with limited energy resources. It is worth noting that the sensors are of two types: threshold monitoring sensors (given black color in Fig. 2) and data monitoring sensors (given blue color in Fig. 2). The first type is triggered by a threshold level to transmit data and second type continuously transmits sensed data. In order to reduce the energy consumption of sensors, a main sensor (MS) is also attached to the bed in one of the scenarios. The MS and sink are assumed to have very high power source as compared to the other sensors. After collecting the sensed data of sensors, the MS forwards these data to the sink which transmits the final information to the external network. From this external network, the doctor is then able to completely know about the patient's conditions. The combination of body sensors and BRs exchange the data in a multi-hop manner.

### 3.2 Types of data reporting

The sensors measure ailments either by continuously monitoring on the basis of time-driven events or on an event-driven basis. The glucose and temperature level monitoring sensors transmit the data whenever the respective levels of these readings either fall below the lower limit or exceed the upper limit (indicating an alarming condition). The low and high temperature levels are set at 35 and 40 °C, respectively. Similarly, the values for the glucose level are 110 and 125 mg/dL, respectively. The rest of the sensors continuously monitor the parameters. Monitoring of variable data types makes this protocol feasible for a wide range of applications like remote monitoring of patients in hospital ward(s) or home(s) suffering from heart diseases, diabetes, drug addiction, etc.

### 3.3 Functionality of the pacemaker

Arrythmia refers to an abnormal heart rhythm due to changes in the conduction of electrical impulses through the heart that are life threatening. The heart may not be able to pump enough blood (least amount of blood needed for proper functioning of different body parts) to the body causing damage to the brain, heart itself, and other organs. Arrythmia can be well controlled by using a pacemaker that creates forced rhythms according to natural human heartbeats which are required for the normal functioning of the heart. The circuitry of a pacemaker consists of a small battery, a generator, and wires attached to the sensor. It senses a heartbeat and sends the signals to the generator through wires. If the heartbeat is not normal, it generates small electrical signals to regulate the heartbeat. The working mechanism of a pacemaker is shown in Fig. 3.

Figure 4 shows the parts of the heart which are attached with the probes of the pacemaker.

### 3.4 Induction link and its parameters

An inductive link consists of two coils, primary and secondary. The primary circuit is powered by a voltage source which generates magnetic flux in order to induce power in the secondary side which is inside the human body as shown in Fig. 5. The skin acts as an interface between the two circuits. The coupling coefficient, $k$, denotes the degree of coupling between the two circuits. In order to avoid damage to the body tissues, the value of $k$ should be less than 0.45. The parameters considered for the validation of the link efficiency are as follows:

- *Voltage gain*: It is the ratio of the output voltage to the input voltage, i.e., $V_{\text{out}}/V_{\text{in}}$.

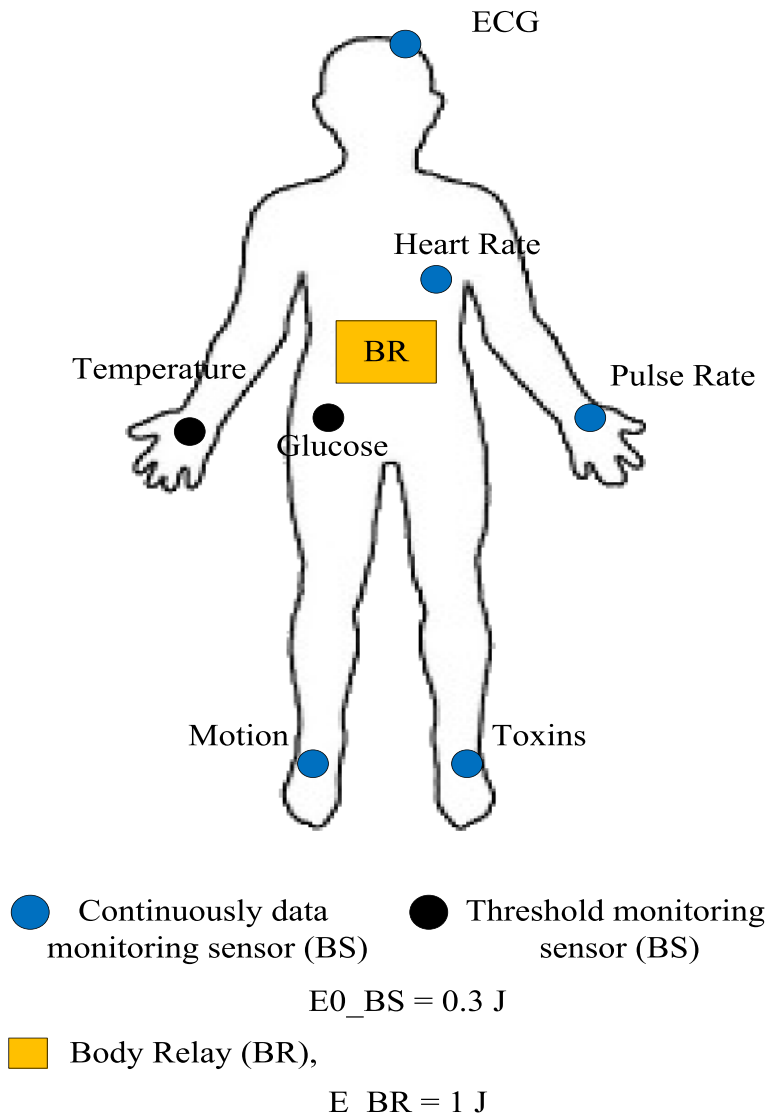


**Fig. 2** Patient scenario

- *Link efficiency* ($\eta$): The ability of transferring power from the primary side to the secondary side is known as the link efficiency.
- *Quality factor*: It is a widespread measure used to characterize resonators. The higher the quality factor, the higher is the resonating effect.

Both voltage gain and $\eta$ depend upon $k$, while quality factor depends upon frequency and load resistor at the secondary side.

## 4 Mathematical model for induction

This section presents a mathematical model for the induction technique which is used to recharge the battery of a pacemaker implanted inside the body to monitor arrhythmic patients. The following subsections discuss the equivalent circuits for induction.

### 4.1 Equivalent circuits

The equivalent circuits are discussed below in the following two subsections.

#### *4.1.1 Series tuned primary circuit (STPC)*

In STPC, a capacitor is connected in series at the primary side. Only a small amount of voltage is induced due to the low coupling factor, i.e., 0.45. So, a series tuned circuit is used to induce sufficient voltage in the secondary coil. The circuit is shown in Fig. 6.

In Fig. 6, $V_s$ is the source voltage, $R_s$ is the series resistance, $C_{1s}$ is the series resonating capacitor at the primary

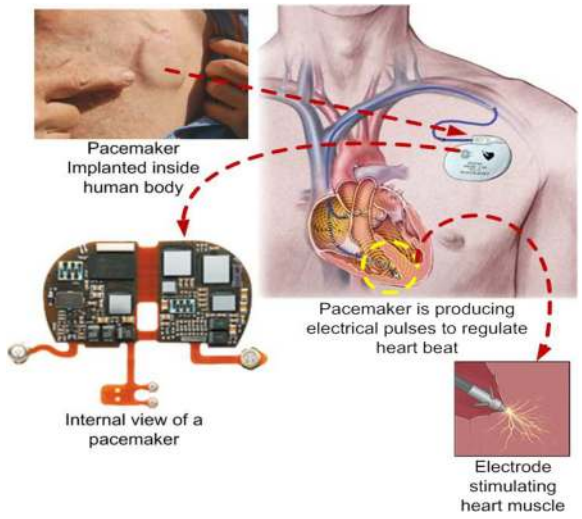


**Fig. 3** Working mechanism of a pacemaker

side, and $L1$ and $L2$ are the inductors at the primary and secondary sides with their series resistances $R_{L1}$ and $R_{L2}$, respectively. $M$ is the mutual inductance, and $R_{\text{load}}$ is the load resistance across which the output voltage $V_{\text{load}}$ is measured. The values of the parameters are shown in Table 1. It is worth mentioning here that these values are adopted from [16].

By applying Kirchoff's voltage law, $V_s$ calculated as follows:

$$V_s = I_1 A - j\omega M I_2. \tag{1}$$

Here, $A = R_s + R_{L1} + j\omega L_1 + \frac{1}{j\omega C_{1s}}$. Similarly, $V_{\text{load}}$ is calculated as follows:

$$V_{\text{load}} = -I_2(j\omega L_2 + R_{L2}) + j\omega M I_1. \tag{2}$$

In order to calculate current in the secondary side "$I_2$", we write the following equation:

$$I_2 = \frac{V_{\text{load}}}{R_{\text{load}}}. \tag{3}$$

By proper substitutions:

$$\frac{V_{\text{load}}}{V_s} = \frac{j\omega M R_{\text{load}}}{AB + \omega^2 M^2}, \tag{4}$$

where, $B = R_{\text{load}} + j\omega L_2 + R_{L2}$. Now, we use the following formula for calculating link efficiency:

$$\eta = \frac{P_2}{P_1} = \frac{V_{\text{load}} I_2}{V_s I_1} = \left(\frac{V_{\text{load}}}{V_s}\right)\left(\frac{I_2}{I_1}\right). \tag{5}$$

After substituting the values of $\frac{V_{\text{load}}}{V_s}$, $I_1$ from Eq. (1) and $I_2$ from Eq. (3), the link efficiency can be written in following form.

$$\eta = \left(\frac{j\omega M R_{\text{load}}}{AB + M^2\omega^2}\right)\left(\frac{V_{\text{load}}}{R_{\text{load}}}\right)\left(\frac{j\omega M R_{\text{load}}}{V_{\text{load}} B}\right). \tag{6}$$

Taking the real part of Eq. (6), $\eta$ becomes:

$$\eta = \frac{\omega^2 M^2 R_{\text{load}}}{Re[B]\left(Re[A]\,Re[B] + \omega^2 M^2\right)}, \tag{7}$$

where, $Re[A] = R_s + R_{L1}$, and $Re[B] = R_{\text{load}} + R_{L2}$. Quality factor for the secondary side is as follows:

$$\text{Quality factor} = \frac{2\pi f L1}{R_{\text{load}}} \tag{8}$$

#### 4.1.2 *Series tuned primary and parallel tuned secondary circuit (STPPTSC)*

The primary side of the circuit in Fig. 7 is the same as the primary side of the series tuned circuit in Fig. 6, except a capacitor $C_{2p}$ is connected in parallel to the secondary

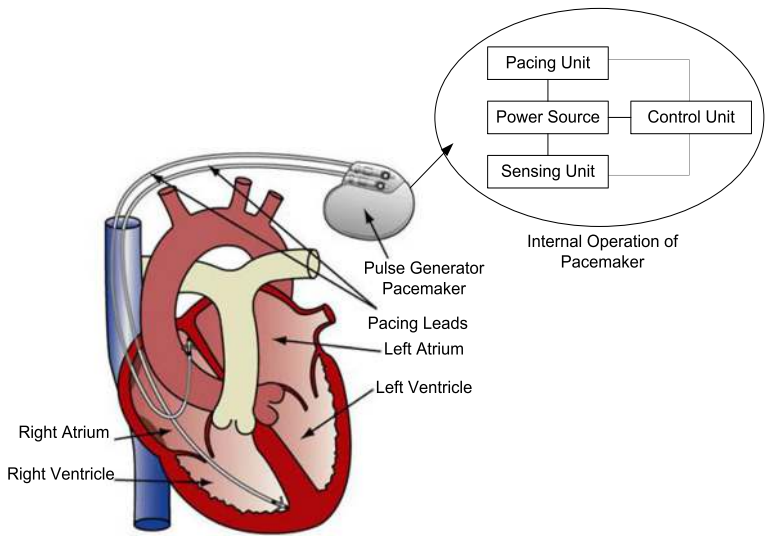


**Fig. 4** Placement of pacemaker's probes inside a human heart

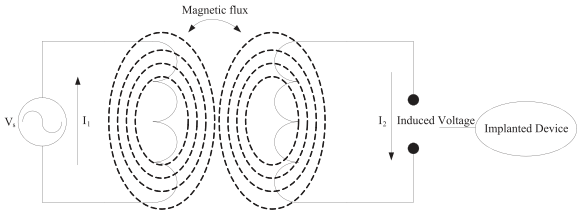


**Fig. 5** Schematic view of an inductive link

side. This parallel capacitor lets the circuit to act as a low pass filter, thereby, preventing damage(s) to body tissues. The circuit is suitable for sensors as these also operate at low frequencies. Moreover, this topology achieves a high voltage gain and a better link efficiency (see Section 6).

The equations for the primary side of the circuit are the same as given for the previous circuit. However, the equations for the secondary side are discussed below. The combined load $Z_{\text{load}}$, is given as

$$Z_{\text{load}} = \frac{R_{\text{load}} - j\omega C_{2p} R_{\text{load}}^2}{1 + \omega^2 C_{2p}^2 R_{\text{load}}^2}. \tag{9}$$

where $R_2$ is the real component and $X_2$ is the reactance of $Z_{\text{load}}$ given as

$$R_2 = \frac{R_{\text{load}}}{1 + \omega^2 R_{load}^2 C_{2p}^2} \tag{10}$$

$$X_2 = -\frac{\omega R_{\text{load}}^2 C_{2p}}{1 + \omega^2 R_{\text{load}}^2 C_{2p}^2}. \tag{11}$$

Now, solving for the voltage at the secondary side,

$$V_{\text{load}} = -I_2(j\omega L_2 + R_{L2}) + j\omega M I_1. \tag{12}$$

Also,

$$V_{\text{load}} = I_{\text{load}} R_{\text{load}} = I_2 Z_{\text{load}}. \tag{13}$$

After proper substitutions, $V_{\text{load}}/V_s$ is written as follows.

$$\frac{V_{\text{load}}}{V_s} = \frac{j\omega M Z_{\text{load}}}{A(Z_{\text{load}} + jwL_2 + R_{L2}) + \omega^2 M^2} \tag{14}$$

**Table 1** Inductive link parameters

| Parameters | Values |
|---|---|
| Operating frequency | $f = 13.56$ MHZ |
| Primary coil | $L_1 = 5.48\mu$H |
| Secondary coil | $L_2 = 1\mu$H |
| Parasitic resistance of the transmitter coil | $R_{L1} \simeq 2.12\Omega$ |
| Parasitic resistance of the receiver coil | $R_{L2} \simeq 1.63\Omega$ |
| Load resistance | $R_{\text{load}} = 320\Omega$ |

For the link efficiency,

$$\eta = \frac{j^2\omega^2 M^2 Z_{\text{load}}}{C(AC + \omega^2 M^2)} \tag{15}$$

where $C = Z_{\text{load}} + j\omega L_2 + R_{L2}$. For the actual consumption at the output, we take the real part of Eq. (13) and avoid the imaginary parts. The final equation for $\eta$ is given as follows:

$$\eta = \frac{\omega^2 M^2 Re[Z_{\text{load}}]}{Re[C]\left(Re[A]\,Re[C] + \omega^2 M^2\right)} \tag{16}$$

where $Re[C] = Re[Z_{\text{load}}] + R_{L2}$ and $Re[Z_{\text{load}}] = R_2$

Quality factor at the secondary side of the circuit is given by:

$$\text{Quality factor} = \frac{2\pi f L_2}{RL_2 + R_{\text{load}}} \tag{17}$$

As flyback diode (placed in reverse biased mode) prevents the voltage surges or spikes into the secondary side, the second induction model is modified by placing a flyback diode in parallel to the primary coil as shown in Fig. 8.

## 5 The proposed routing protocols

The DARE protocol aims to monitor patients in a heterogeneous network while reducing the energy consumption of the monitoring sensors by deploying a relay node. The

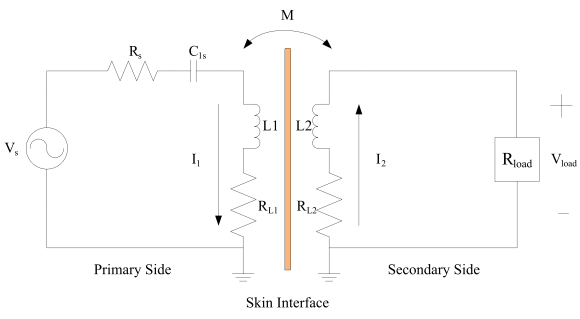


**Fig. 6** STPC

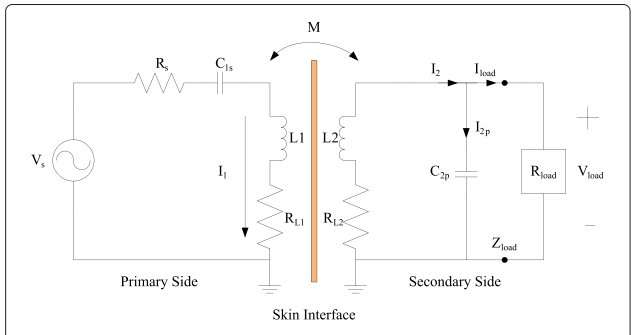


**Fig. 7** STPPTSC

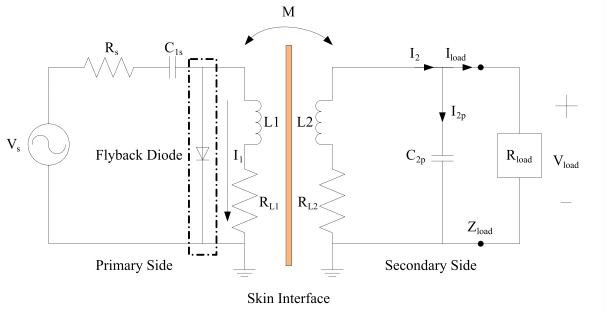


**Fig. 8** STPPTSC with flyback diode

relay node reduces the communication distance between the sender and the receiver. The monitored data travels through the hierarchy of sensors towards the destination node to avoid the battery of sensors to discharge at an earlier stage. The following subsections separately discuss the network topology, types of data, and communication flow in detail.

### 5.1 Communication flow of DARE protocol

Information sharing is necessary for WBASNs because the newly implanted/affixed sensors are in a state of missing reliable communication infrastructure. Therefore, the network configurations are upgraded periodically. We use a HELLO message exchange technique to inform each sensor with the IDs of other sensors, coordinates of all other nodes, status of links, and received signal strength. Sensor node with initial energy greater than zero is considered as alive. The node types are determined via their IDs. During the centralized protocol operation, eight patients are independently monitored. For each patient, each of the body sensors conveys information to the corresponding in range body relay which is equipped with higher energy resources. The received data is finally transmitted to the MS. The protocol's flow chart is shown in Fig. 9.

The algorithm for patient monitoring is as follows:

- First, the body sensor is checked whether it is alive or not. If yes, then the algorithm checks for the body relay to be alive. If the body sensor is found alive, then it checks whether it is a threshold measuring sensor or a continuous data monitoring sensor.
- If the body sensor is a threshold measuring sensor, it checks if the low or high threshold levels are reached. If yes, then it measures the distance between that body sensor and body relay.
- Afterwards, it calculates the energy consumption costs in the transmission process and in the reception process for the body sensor and the body relay, respectively.

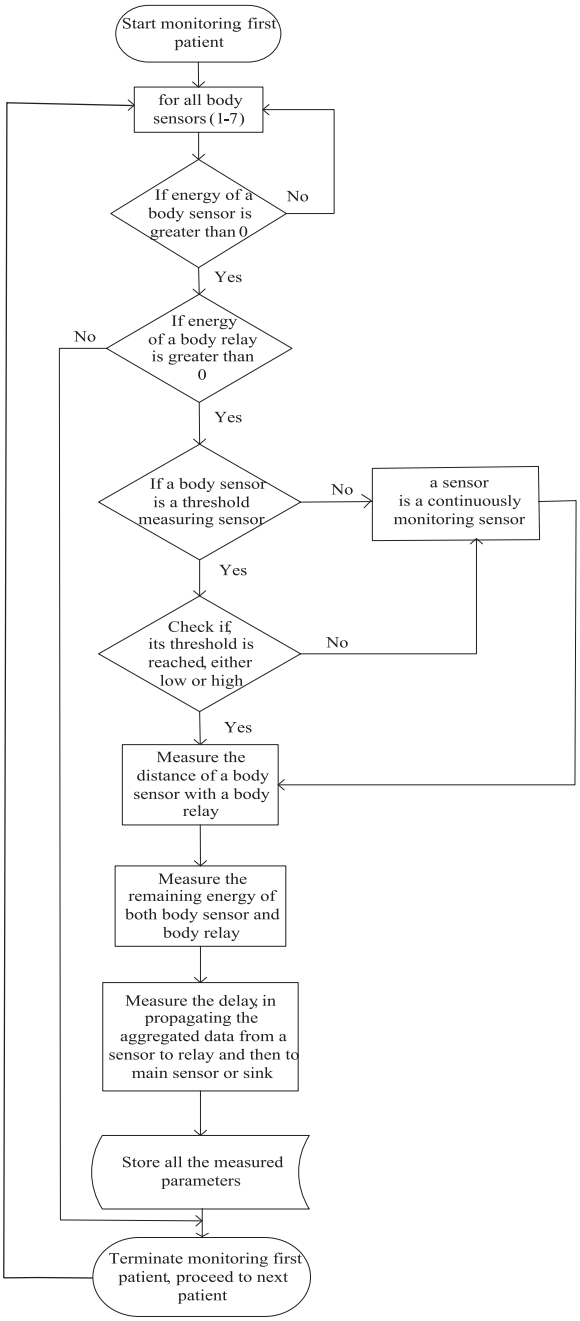


**Fig. 9** Flow chart of DARE protocol

- Then, it estimates the delay in propagating the data from the body sensor to the body relay.
- If the threshold is not reached, then the algorithm proceeds to check the other body sensors in the same manner and calculates the distance, remaining energy, and delay. Finally, the estimated parameters are separately stored in different variables.
- This whole process continues till all the body sensors are checked.

- When the body relay receives data from all the sensors, it aggregates the received data and transmits these data either directly to sink (static or mobile) or MS, depending upon the particular scenario.
- After the data aggregation phase, the transmission and remaining energy of the body relay is calculated. The remaining energy is given as

$$\text{Remaining energy} = \text{Initial energy} - \text{Transmission energy} \tag{18}$$

- After checking all the sensors of the first patient, the protocol operation advances towards checking the next patient.

### 5.2 Mobility in DARE

The DARE protocol also considers mobility of the patient's legs, arms, and head to account for bed patients. We have considered four different positions for each arm, three different positions for each leg, and head for all the patients as shown in Fig. 10b–e. In Fig. 10b–e, the dashed arrows and dashed spheres illustrate the relative movement horizon in each posture for each arm, each leg, and head (note: spheres are replaced by circles/ellipses only for the sake of simplicity in drawing).

### 5.3 The MI-DARE routing protocol

The continuous data monitoring sensors monitor/scan the parameter of interest regularly. Since not all the scanned data is necessarily important to be transmitted, i.e., the scanned data if similar to the previously sent data does not contain useful information and is considered as redundant data. Transmission of redundant data leads to surplus energy consumption cost which ultimately leads to network lifetime degradation. Thus, the objective here

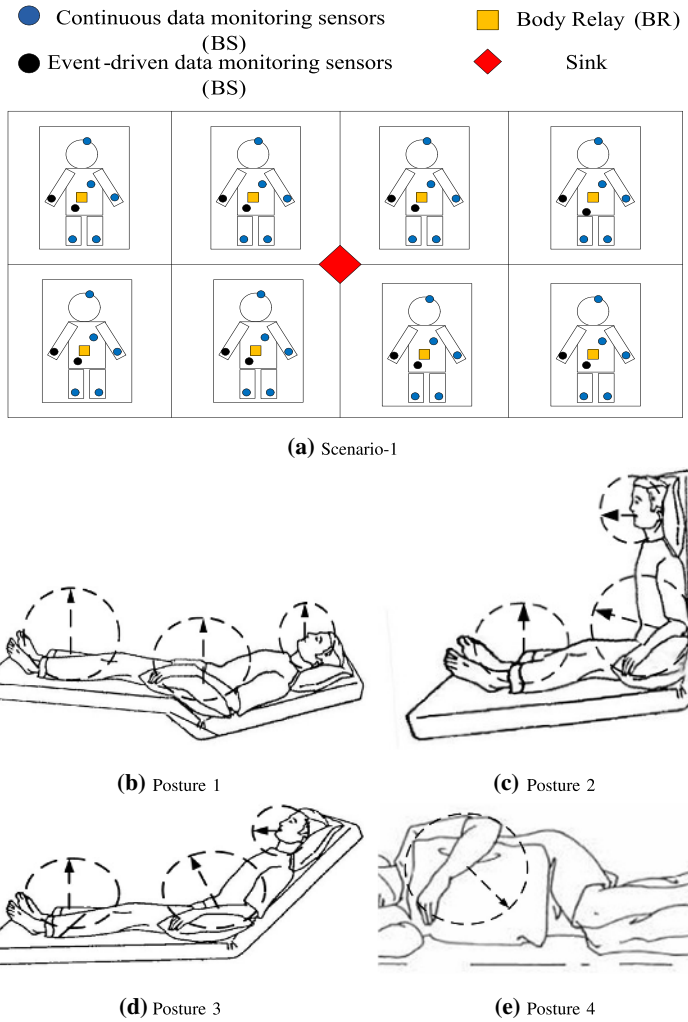


**Fig. 10 a** sink is placed at the center of the ward. Body sensors on different patients carry information and transmit to their respective body relay which then aggregates and relays the received data to sink. The communication flow is from body sensors → body relays → sink. **b**–**e** mobility postures

is to improve the network lifetime of DARE protocol by removing this redundancy. In order to do this, we use the MI-based technique here.

MI tells us how one random variable (sensor reading) is close to another. Let $I$ be the scanned input of sensor node at time $t_1$, and $J$ be the scanned input of sensor node at time $t_2$. We calculate the MI between current value say $J$ with its previous value say $I$ as follows [37]:

$$MI(I,J) = \sum_i \sum_j p\left(I_i, J_j\right) \log_2 \left( \frac{p\left(I_i, J_j\right)}{p(I_i)p(J_j)} \right) \quad (19)$$

where $p(I_i, J_j)$ is the joint probability distribution function between $I_i$ and $J_j$ and $p(I_i)$ and $p(J_j)$ are the independent probability functions of $I_i$ and $J_j$, respectively. This equation gives us very useful information: (i) the MI value is high if $I$ and $J$ have similar information content, (ii) the MI value is zero if $I$ and $J$ are independent, and (iii) the MI is neither high nor zero if the information content between $I$ and $J$ is loosely related. Based on this calculation, the proposed MI-DARE protocol checks the information content of the current sensed data of continuous data monitoring sensor. If the information content of current sensed data is found similar to that of the previously sensed data, then the current sensed data is not transmitted. In this way, surplus energy consumption cost due to redundant transmissions of continuous data monitoring sensors is prevented which leads to prolongation of the network lifetime.

## 6 Experimental results and discussions

This section discusses the simulation results for the inductive link model and the DARE and the MI-DARE protocols. The protocol considers five different scenarios by having the same topology for body sensors and body relays. Mobility considerations are as per Section 6.2. The sink is either mobile or static depending on scenarios illustrated in Figs. 10, 11, 12, 13, and 14. Different positions of sink in scenarios 2 and 5 are shown in Table 2.

The basic radio model proposed for WBASNs is in [26]. We choose the radio model of [26] due to two reasons: (i) this model meets all the design considerations of our work and (ii) it is the mostly used one in literature. To transmit "w" bit data over a distance "d", the dissipated energy of transmitter $E_{tx}(w,d)$ is given by the following equation:

$$E_{\text{tx}}(w,d) = E_{\text{TXelec}} \times w + \varepsilon_{\text{amp}} n \times w \times d^n. \quad (20)$$

where, $E_{\text{TXelec}}$ represents the per bit energy consumption to run the circuitry of transmitter, $n$ is the path loss (PL) exponent, and $\varepsilon_{\text{amp}}$ represents the amplification factor. The value of $n$ for line of sight (LOS) communication is 3.38 and for non-LOS communication its value is 5.9. It is worth mentioning here that DARE protocol assumes LOS communication between sensors. Equation for the reception energy is given as follows.

$$E_{\text{rx}}(w) = E_{\text{RXelec}} \times w \quad (21)$$

where $E_{\text{RXelec}}$ represents the per bit energy consumption to run the circuitry of receiver. For simulation purpose, numerical values of all the parameters of the radio model are shown in Table 3.

### 6.1 The mathematical model

In order to evaluate the inductive link model in Section 6, we choose three performance metrics: voltage gain, link efficiency, and quality factor.

#### *6.1.1 STPC*

The results are shown and discussed below.

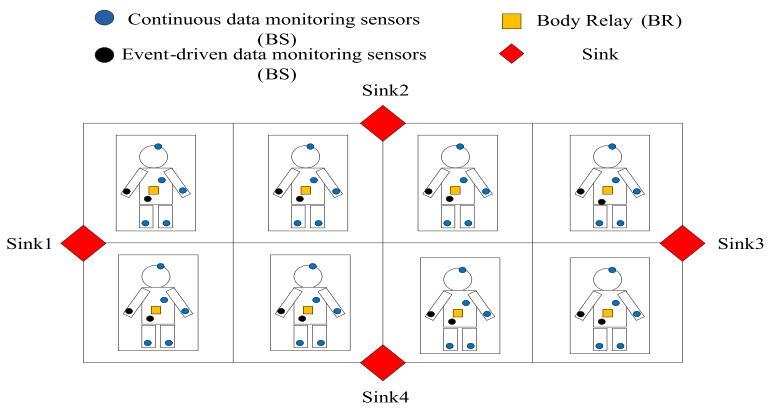


**Fig. 11** Scenario 2: four sinks are separately placed in the center of the walls. The body sensors of each patient transmit data to their respective body relay. The body relay checks for the nearest sink and communicate with it. This helps in reducing the communication distance as well as the burden over body relays in terms of utilizing their energy resources. The communication flow is body sensors → body relay → (Sink1 or Sink2 or Sink3 or Sink4)

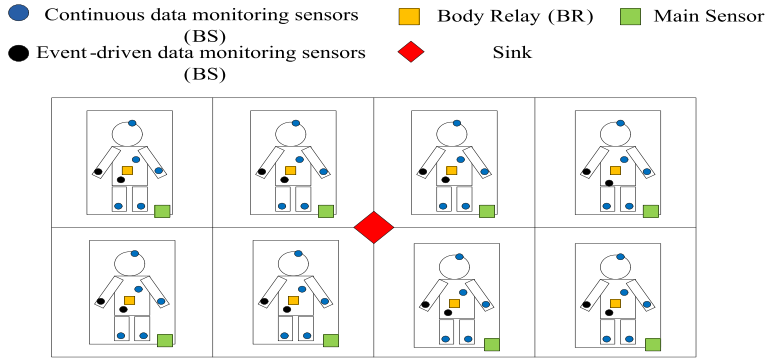


**Fig. 12** Scenario 3: MS is affixed on each bed. MS has more energy resources which makes it a powerful device as compared to body sensors and body relays. The placement of MS helps the body relay to consume less energy, as body relay transmits data over shorter distance. However, this scenario increases the propagation delay. Communication flow is body sensors → body relay → MS → sink

- *Voltage gain:* From the equation for voltage gain, $V_{\text{load}}/V_s$ for STPC is directly proportional to $R_{\text{load}}$. In Fig. 15, when the value of $k$ increases from 0.2 to 0.8, $V_{\text{load}}/V_s$ also increases. For every value of $k$, $V_{\text{load}}/V_s$ shows almost a linear response as $R_{\text{load}}$ increases from 0 Ω to 100 Ω.
  For $k = 0.4$ and $R_{\text{load}} = 320\ \Omega$, $V_{\text{load}}/V_s = 2.2$. We have chosen the aforementioned values of $k$ and $R_{load}$ because these make the circuitry harmless to human tissues.
- *Link efficiency:* It is clear from Fig. 16 that the value of the link efficiency is highly dependent on $k$. For $k = 0.4$ and $R_{\text{load}}$, the value of $\eta$ is 0.75.

#### 6.1.2 STPC and STPPTC

Results for STPC and STPPTC are shown and discussed below.

- *Voltage gain:* In Fig. 17, changes in the voltage gain $V_{\text{load}}/V_s$, by varying $R_{\text{load}}$ for STPC and STPPTC are shown. It is clear from the figure that changes in $R_{\text{load}}$ do not produce any significant change in $V_{\text{load}}/V_s$. The only noticeable increase in $V_{\text{load}}/V_s$ is produced by increasing $k$. However, due to the fact that this link is used on human body to induce voltage to the implanted device, the value of $k$ changes only from 0 to 0.45. From $R_{\text{load}} = 0\Omega$ to 100 Ω, the behavior of

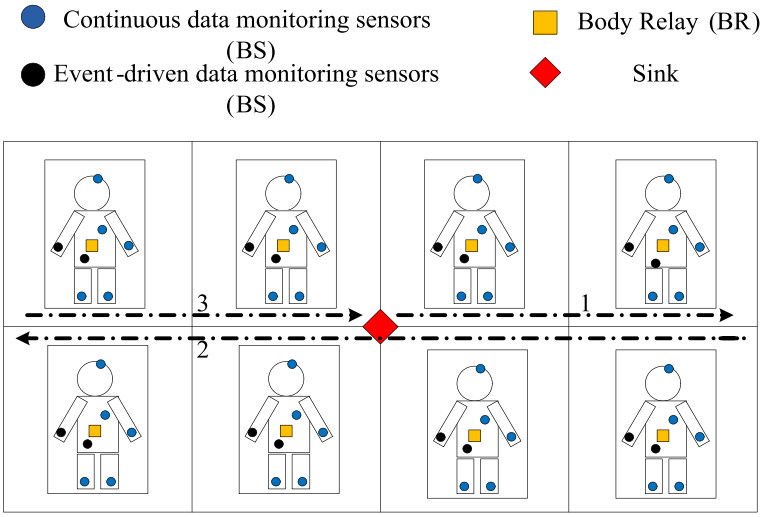


**Fig. 13** Scenario 4: The sink is made mobile along the center of the ward. The sink first starts moving from center towards the right wall. Afterwards, it comes back towards the center and moves towards the left wall. Then again move towards the center. This happens throughout the network lifetime. The sink mobility helps the body relay to consume less energy in some cases while more in some other cases. It also has a significant impact over the propagation delay. The communication flow is the same as for scenario 1

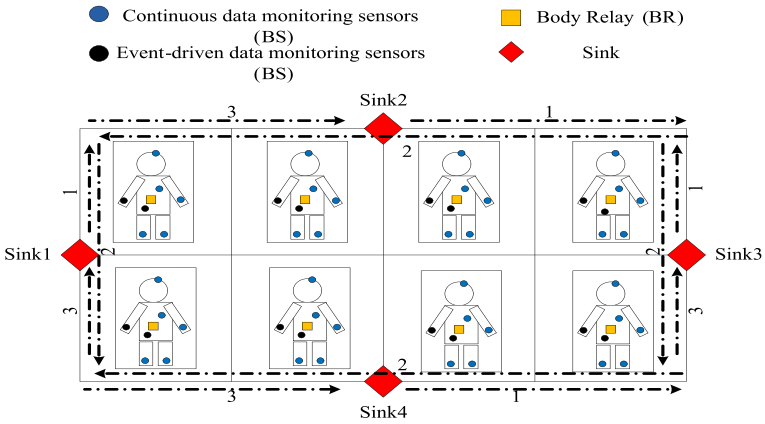


**Fig. 14** Scenario 5: It assumes the same topology as in scenario 2; however, now all the four sinks are made mobile around the walls of the ward. All the sinks start moving from center of the wall, then move in one direction, come back towards the center and then move in the opposite direction and finally come back again towards the center. The sinks move altogether. This combined movement facilitates the body relays of all the patients to consume less energy consumption as compared to all the other scenarios. This is due to decrease in the communication range between the body relay and sinks. Mobility of multiple sinks helps in increasing the network lifetime and reducing the delay in transmitting the data. In this scenario, each of the body relays communicates with the minimum distant sink. The communication flow is body sensors to body relay to the nearest moving sink (Sink1 or Sink2 or Sink3 or Sink4)

$V_{\text{load}}/V_s$ is nearly constant. After reaching 100 Ω, it increases almost linearly. For $k = 0.4$ and $R_{\text{load}} =$ 320 Ω, the voltage gain is about 3.7. Hence, the value of $V_{\text{load}}/V_s$ is significantly higher, when the secondary circuit is tuned in parallel as compared to the tuning of the primary circuit. Moreover, the output voltage is nearly four times higher than the driving input voltage.

- *Link efficiency:* The link efficiency graph for STPPTSC is shown in Fig. 18. For every value of $k$, this figure depicts the steepness of the link efficiency till $R_{\text{load}} = 100$ Ω. After this value, the link efficiency of the circuit becomes constant. For $k = 0.4$ and $R_{\text{load}}$ = 320 Ω, the link efficiency is about 0.9, i.e., 90 %. In comparison to the STPC, the link efficiency of the parallel tuned secondary circuit increases by 15 %. In other words, 90 % of the input power is efficiently transferred to the secondary side.
- *Quality factor*: Fig. 19 shows the comparison plot of quality factor for both the equivalent circuits. It is clear from the figure that quality factor increases as the operating frequency is increased. For the safety of body tissues, the frequency is set to be 13.56 MHz. The quality factor of STPPTSC is higher than the other circuit which means that the second equivalent circuit achieves good tuning under resonant conditions.

Figure 20 shows the merits of STPPTSC over STPC with respect to three parameters: voltage gain, link efficiency, and quality factor.

### 6.2 DARE and MI-DARE protocols

DARE, MI-DARE, and M-ATTEMPT protocols are compared by taking mobility of the patients into consideration. We investigate different parameters including stability period, network lifetime, number of packets sent, number of received packets at sink, number of dropped packets, and propagation delay. The simulation parameters are listed in Table 2. During the simulation setup, nodes cease transmitting data packets when their energy is completely

**Table 2** Locations of multiple sinks in the hospital ward

| Sink | Position | |
|---|---|---|
| | x (m) | y (m) |
| Sink1 | 0 | 3 |
| Sink2 | 6 | 6 |
| Sink3 | 12 | 3 |
| Sink4 | 6 | 0 |

**Table 3** Parameters of energy model

| Parameter | Value |
|---|---|
| $E_{\text{TXelec}}$ | 16.7 nJ/bit |
| $E_{\text{RXelec}}$ | 36.1 nJ/bit |
| $E_{\text{amp}}$ | 1.97 nJ/bit |
| $E_{\text{amp}}$ | 7.99 nJ/bit |
| $n$ for LOS | 3.38 |
| $n$ for non-LOS | 5.9 |
| $w$ | 4000 bits |

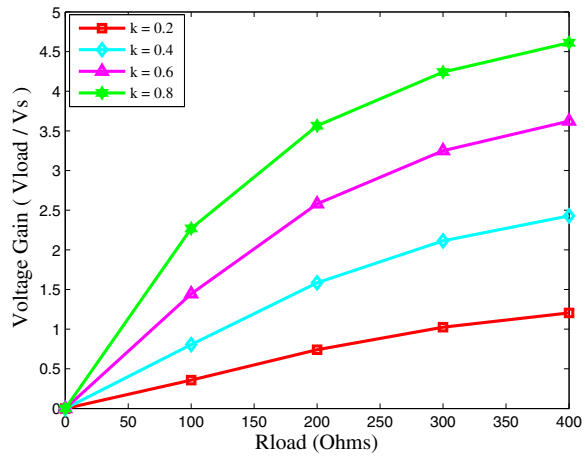


**Fig. 15** Voltage gain of STPC

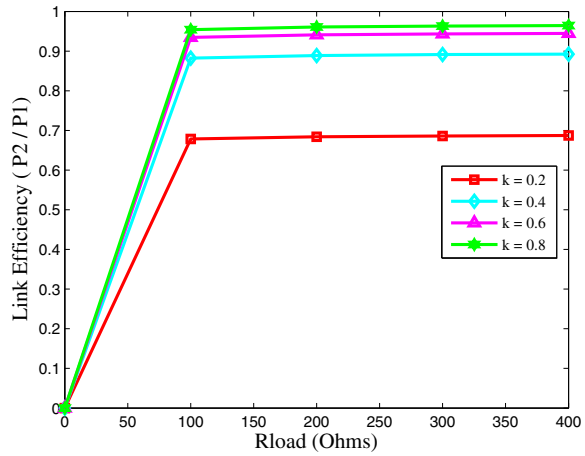


**Fig. 18** Link efficiency of STPPTSC

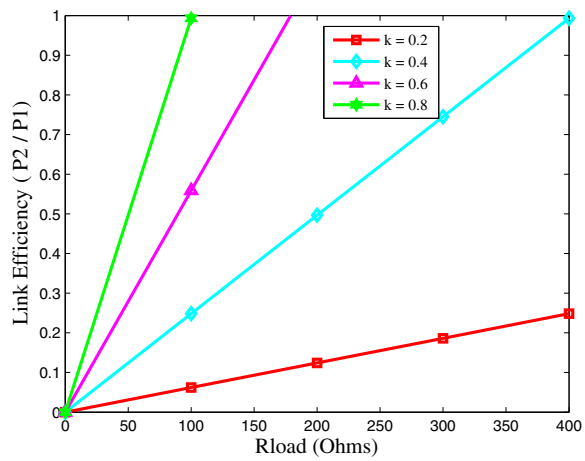


**Fig. 16** Link efficiency of STPC

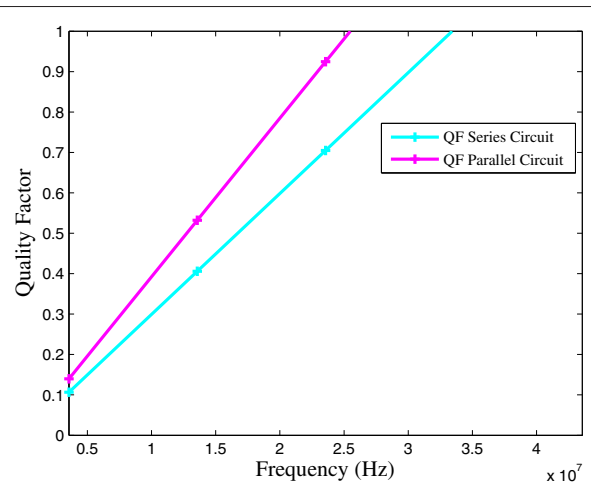


**Fig. 19** Quality factor

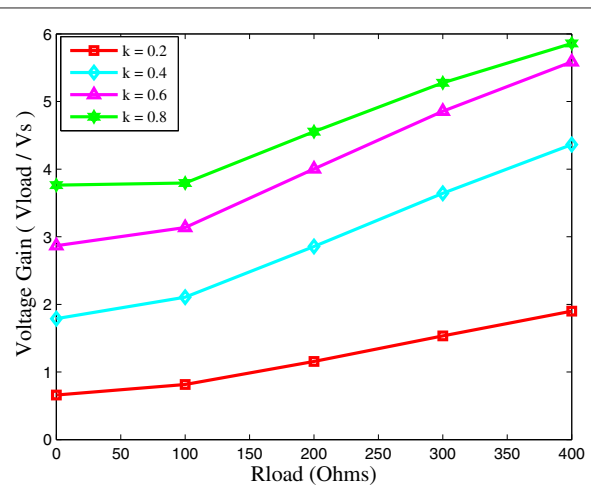


**Fig. 17** Voltage gain of STPPTSC

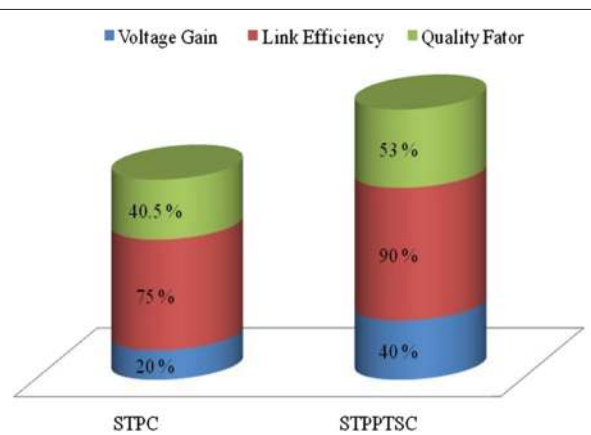


**Fig. 20** Comparison results between STPC and STPPTSC

depleted. The similarities and differences between the two protocols in terms of topology, technical parameters, communication type, etc. are tabulated in Table 4.

#### *6.2.1 Stability period and network lifetime*

The time from the establishment of the network till the death of the first node is known as the stability period. Similarly, the time from the establishment of the network till the death of the last node is known as the network lifetime.

**Table 4** Similarities and differences between DARE and M-ATTEMPT

| Parameter | DARE | M-ATTEMPT |
|---|---|---|
| Types of devices | Body sensors | Sensors |
| | Body relay | Sink |
| | Main sensor (MS) | |
| | Sink | |
| Deployment | Body sensors, body relays, and MS are fixed | Sensors and sink both are fixed |
| | Sink can either be static or mobile | |
| Topology per patient | 7 body sensors | 7 sensors |
| | 1 body relay on chest | 1 sink on chest |
| Communication flow | Scenario 1: body sensors to body relays to sink | Sensors to sink or sensors to other sensors to sink |
| | Scenario 2: body sensors to body relay to nearest sink | |
| | Scenario 3: body sensors to body relay to MS to sink | |
| | Scenario 4: body sensors to body relay to moving sink | |
| | Scenario 5: body sensors to body relay to nearest moving sink | |
| Energy parameters | $E0_{BSs} = 0.3J$ | $E0_{sensors} = 0.3$ J |
| | $E0_{BR} = 1J$ | $E_{Sink} =$ infinite |
| | $E_{MS} =$ infinite | |
| | $E_{Sink} =$ infinite | |
| Network type | Heterogeneous in terms of energy of body sensors and body relays | Homogeneous in terms of energy of sensors |
| Communication type | Multi-hop | Single-hop |
| | | Multi-hop |
| Types of data reporting | Event-driven | Event-driven |
| | Time-driven | Time-driven |

From Fig. 21, it is clear that the stability period in M-ATTEMPT is about 239 rounds. Whereas, in DARE, it is 859, 1027, 1150, 1437, and 1496 for scenarios 1, 2, 3, 4, and 5, respectively. Similarly, in MI-DARE; the stability period is 1033, 1378, 1727, 1239, and 1800 for scenarios 1, 2, 3, 4, and 5, respectively. In DARE, as soon as the first node dies, the other nodes also die very quickly. This means that DARE protocol ensures uniform load on all the nodes. The MI-DARE does not transmit redundant data. It means that sufficient amount of energy consumed during transmission is saved which ultimately leads to enlarged stability period and prolonged network lifetime. On average, the MI-DARE achieves of about 20 % network lifetime prolongation as compared to DARE.

When multiple moving sinks are deployed as per scenario 5, the nodes (both body sensors and body relays) survive for increased number of rounds, i.e., about 3345 rounds. This is because of the deployment of multiple sinks at different locations which facilitates the body relays to transmit data at relatively shorter distances. This topology significantly helps the body relays to stay alive for some additional rounds. Among all the presented scenarios, scenario 5 shows the greatest stability period and network lifetime. The MS in scenario 3, attached with the bed, enables body relays to die with decreased rate as compared to the other scenarios. In scenario 1, as the sink is static, all the nodes remain alive till 858 rounds. This scenario has the least stability period as compared to the other scenarios. Due to appropriate deployment of body relays, the body sensors continue to send their data. Accordingly, the network lifetime significantly increases. Figure 21 also shows that the nodes in M-ATTEMPT rapidly consume energy as compared to the nodes in DARE. There is a sharp fall-off in the energy consumption of the nodes following M-ATTEMPT routing protocol, thereby, dying at an earlier stage. On the other hand, the nodes in DARE protocol consume minimum energy because these are facilitated by body relays.

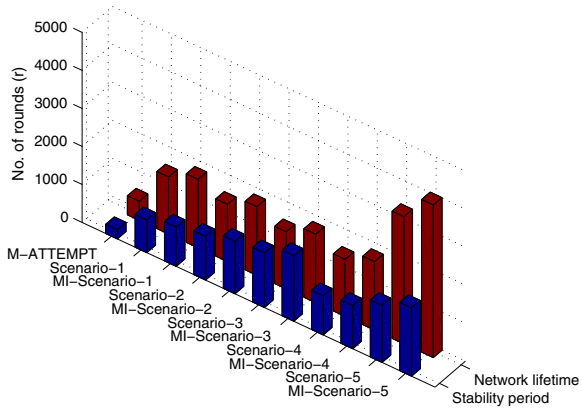


**Fig. 21** Stability period and network lifetime (S=Scenario)

#### *6.2.2 Throughput*

Figure 22 shows that among M-ATTEMPT, and all the scenarios of DARE and MI-DARE, scenario-5 of DARE and MI-DARE has maximum number of packets sent to the sink. This is due to the relative prolonged lifetime of sensors. Due to mobility and introduction of body sensors and MS, the communication distance is significantly reduced which means minimized energy consumption. This leads to prolonged network lifetime which ultimately increases the number of transmitted packets. From Fig. 22, it is seen that more number of packet transmission rate in scenario 5 increases the probability of packet drop rate. This figure also shows that the dropped packets are the highest in scenario 5, whereas, these are the lowest in M-ATTEMPT because more number of sensors die at an earlier stage, so, less number of packets are dropped in the network. While receiving packets, the probability of sensors is 0.7. In scenario 5, the network lifetime is prolonged due to sink mobility. DARE proves to have more throughput than that of M-ATTEMPT as evident from Fig. 22. On the other hand, the number of packets sent, dropped, and received in MI-DARE are less than that of DARE when relatively compared in terms of scenarios from 1 to 5. These results show 10 % decrease in throughput for MI-DARE in comparison to DARE. Unlike DARE, sensors in MI-DARE do not send redundant packets to sink leading to decreased number of packets that are sent by source nodes, dropped due to bad channel conditions, and received at the sink. An interesting fact here is the packet delivery ratio, which on average is the same for DARE and MI-DARE. This means that MI-DARE does not pay the cost of packet delivery ratio to achieve network lifetime prolongation.

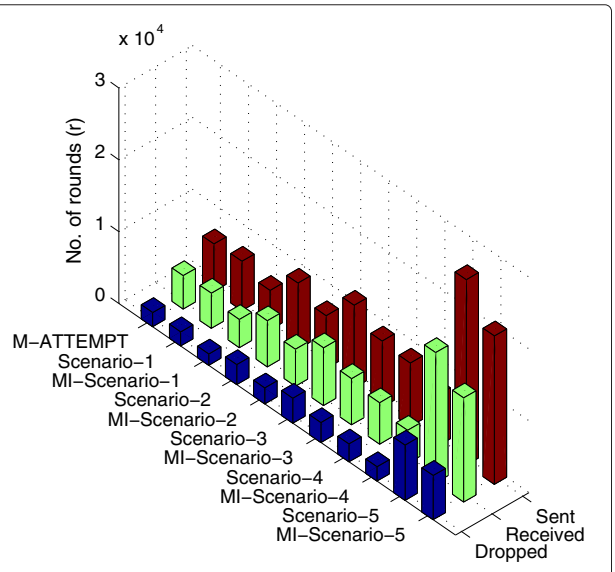


**Fig. 22** Number of packets: sent, dropped, and received (S=Scenario)

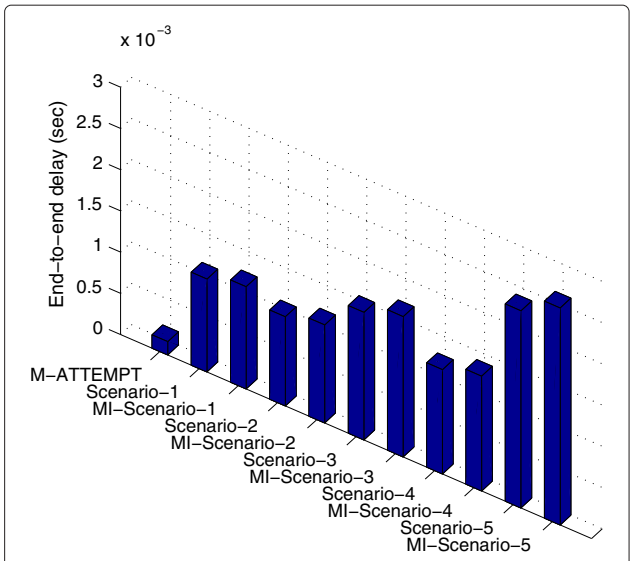


**Fig. 23** End-to-end delay (S = Scenario)

#### *6.2.3 End-to-end delay*

In scenario 3, a packet propagates through a long route from the body sensors to the sink. The facility of multiple static sinks decreased the delay as is in the case of scenario 2 (see Fig. 23.) In case of the proposed protocol DARE, the delay continues to increase somewhat linearly for some initial rounds, after which it becomes constant. The lowest end-to-end delay makes the M-ATTEMPT protocol favorable for applications where huge delay cannot be tolerated. The reason for minimum delay is the attachment of body relay at the chest of the patient which significantly minimizes the communication distance. Hence, the proposed DARE protocol achieves energy efficiency at the cost of relatively high end-to-end delay. Now, let us compare DARE with MI-DARE in terms of end-to-end delay, the later one takes 8 % more time in comparison to the former one. The reason for the relatively high end-to-end delay of MI-DARE is the processing time required for the MI technique.

Table 5 shows the comparison between MI-DARE, DARE, and M-ATTEMPT with respect to the given network performance parameters.

**Table 5** Comparison results between MI-DARE, DARE, and M-ATTEMPT

| Metric | MI-DARE | DARE | M-ATTEMPT |
|---|---|---|---|
| Stability period | Highest | Moderate | Least |
| Network lifetime | Highest | Moderate | Least |
| Energy consumption | Least | Moderate | Highest |
| Packet delivery ratio | High | High | Moderate |
| End-to-end delay | Highest | High | Least |

## 7 Conclusions

This paper focuses on two aspects. One is the modeling of an inductive link, and the other is the proposition of an energy-efficient routing protocol. The induction mechanism (modeling part) is used to recharge the battery of the in-body pacemaker. Simulation results show that the STPPTSC achieves good results for voltage gain, link efficiency, and quality factor as compared to STPC. The circuit achieves about *four times* higher output voltage than the driving input voltage and the link efficiency. The routing part deals with the design and comparison of the proposed protocol with an existing protocol, M-ATTEMPT. Being able to monitor data continuously or when a certain threshold is reached, the newly proposed protocol DARE proved to be more versatile than M-ATTEMPT. By introducing the MS and the body relay in the network, the proposed protocol showed relatively better performance in terms of energy consumption. Moreover, DARE also considered mobility caused by different postural changes off the patient's body and achieved better results than M-ATTEPMT. Unlike M-ATTEMPT and DARE, MI-DARE does not transmit redundant packets which ultimately leads to prolonged network lifetime, however, at the cost of end-to-end delay. M-ATTEMPT shows the least end-to-end delay in comparison to DARE and MI-DARE which makes it preferable for delay sensitive applications.

The authors in [38] derived analytical channel model and propagation characteristics of arm motion as a spherical model. Future work includes the proposition of a mathematical model for the induction technique used to recharge the sensors through an electric field which is produced due to the arm movement of a human body. We are also very much interested in the real-time experimental test bed implementation of our proposed techniques. Moreover, intelligent routing of data messages via swarm optimization technique like [39] and energy-aware quality of service routing like [40] are also under consideration. We are also interested in expanding our research horizon to cooperative medium access control protocol for WBASNs [41].

**Competing interests**
The authors declare that they have no competing interests.

**Acknowledgements**
The authors would like to extend their sincere appreciation to the Deanship of Scientific Research at King Saud University for funding this research through Research Group Project NO. (RG#1435-051).

**Author details**
[1]COMSATS Institute of Information Technology, Islamabad, Pakistan. [2]Institute of Space Technology, Islamabad, Pakistan. [3]College of CIS, King Saud University, Almuzahmiah, Saudi Arabia. [4]Department of Electrical and Computer Engineering, University of Idaho, Moscow, ID, USA. [5]CIS, Higher Colleges of Technology, Fujairah Campus, Fujairah, United Arab Emirates. [6]University of Alberta, Alberta, Canada.

Received: 2 December 2015 Accepted: 23 May 2016
Published online: 13 June 2016

**References**

1. E Kartsakli, AS Lalos, A Antonopoulos, S Tennina, MD Renzo, L Alonso, C Verikoukis, A survey on M2M systems for mHealth: a wireless communications perspective. Sensors. **14**(10), 18009–18052 (2014)
2. J Ben-Othman, K Bessaoud, A Bui, L Pilard, Self-stabilizing algorithm for efficient topology control in wireless sensor networks. J. Comput. Sci. **4**(4), 199–208 (2013)
3. N Raveendranathan, S Galzarano, V Loseu, R Gravina, R Giannantonio, M Sgroi, R Jafari, G Fortino, From modeling to implementation of virtual sensors in body sensor networks. Sensors J. IEEE. **12**(3), 583–593 (2012)
4. VN Talooki, J Rodriguez, H Marques, Energy efficient and load balanced routing for wireless multihop network applications. Int. J. Distrib. Sensor Netw. **2014**. 13. Article ID 927659. doi:10.1155/2014/927659
5. J-J Liaw, C-W Chou, C-Y Dai, The lifetime extension of wireless sensor networks using adaptive energy allocation by distance. Int. J. Distrib. Sensor Netw. **2013**, 8 (2013). article ID 982573. doi:10.1155/2013/982573
6. H Huo, X Xu, H Zhang, YH Chuang, T-C Wu, Wireless sensor networks based healthcare system: a survey on the view of communication paradigms. Int. J. Ad Hoc Ubiquitous Comput. **8**(3), 135–154 (2011)
7. KM Silay, C Dehollain, M Declercq, Inductive power link for a wireless cortical implant with two-body packaging. Sensors J. IEEE. **11**(11), 2825–2833 (2011)
8. P-V Mekikis, A Lalos, A Antonopoulos, L Alonso, C Verikoukis, Wireless energy harvesting in two-way network coded cooperative communications: a stochastic approach for large scale networks. Commun. Lett. IEEE. **18**(6), 1011–1014 (2014)
9. P-V Mekikis, A Antonopoulos, E Kartsakli, A Lalos, L Alonso, C Verikoukis, Information exchange in randomly deployed dense WSNs with wireless energy harvesting capabilities. Wireless Commun. IEEE Trans. **99**, 1–1 (2016). doi:10.1109/TWC.2016.2514419
10. E Ibarra, A Antonopoulos, E Kartsakli, JJ Rodrigues, C Verikoukis, QoS-aware energy management in body sensor nodes powered by human energy harvesting. Sensors J. IEEE. **16**(2), 542–549 (2016)
11. A Djouama, L Mokdad, M Abdennebi, Performance evaluation of lifetime-driven admission control for infrastructure-less clustered wireless networks. Concurrency Comput. Prac. Exp. **25**(5), 718–727 (2013)
12. S Yousaf, N Javaid, U Qasim, N Alrajeh, ZA Khan, M Ahmed, Towards reliable and energy-efficient incremental cooperative communication for wireless body area networks. Sensors. **16**(3), 1–22 (2016)
13. E Reusens, W Joseph, B LatrÂt'e, B Braem, Vermeeren G, E Tanghe, L Martens, I Moerman, C Blondia, Characterization of on-body communication channel and energy efficient topology design for wireless body area networks. Inform. Technol. Biomed. IEEE Trans. **13**(6), 933–945 (2009)
14. J Elias, A Mehaoua, in *Communications (ICC), 2012 IEEE International Conference*. Energy-aware topology design for wireless body area networks (IEEE, Ottawa, ON, 2012), pp. 3409–3410
15. H Ali, TJ Ahmad, SA Khan, Mathematical modeling of an inductive link for optimizing efficiency. Ind. Electron. Appl. ISIEA 2009, IEEE Symp. **2**, 831—835 (2009)
16. GB Hmida, H Ghariani, M Samet, Design of wireless power and data transmission circuits for implantable biomicrosystem. Biotechnology. **6**(2), 153–164 (2007)
17. H Ali, TJ Ahmad, SA Khan, Inductive link design for medical implants. Ind. Electron. Appl. ISIEA IEEE Symp. **2**, 694–699 (2009)
18. PV Mekikis, E Kartsakli, AS Lalos, A Antonopoulos, L Alonso, C Verikoukis, in *IEEE International Conference on Communications (ICC)*. Connectivity of large-scale WSNs in fading environments under different routing mechanisms, (London, 2015), pp. 6553–6558
19. N Javaid, Z Abbas, MS Fareed, ZA Khan, N Alrajeh, M-attempt: a new energy-efficient routing protocol for wireless body area sensor networks. Procedia Comput. Sci. **19**, 224–231 (2013)
20. A Tauqir, S Akram, A Khan, N Javaid, M Akbar, in *8th IEEE International Conference on Broadband and Wireless Computing, Communication and Applications (BWCCA13)*. Non-invasive induction link model for implantable biomedical microsystems: pacemaker to monitor arrhythmic patients in body area networks (IEEE, Compiegne, 2013)

21. A Tauqir, N Javaid, S Akram, A Rao, S Mohammad, in *8th International Conference on Broadband and Wireless Computing, Communication and Applications (BWCCA13)*. Distance aware relaying energyefficient: dare to monitor patients in multi-hop body area sensor networks (IEEE, Compiegne, 2013)
22. A Darwish, AE Hassanien, Wearable and implantable wireless sensor network solutions for healthcare monitoring. Sensors. **11**(6), 5561–5595 (2011)
23. F Burny, M Donkerwolcke, F Moulart, R Bourgois, R Puers, K Van Schuylenbergh, M Barbosa, O Paiva, F Rodes, J Begueret, et al., Concept, design and fabrication of smart orthopedic implants. Med. Eng. Phys. **22**(7), 469–479 (2000)
24. PK Pothuri, DL Ranganathan, V Sarangan, S Radhakrishnan, Energy-efficient routing in wireless sensor networks for delay sensitive applications. Int. J. Ad Hoc Ubiquitous Comput. **5**(2/2010), 103–116 (2010). doi:10.1504/IJAHUC.2010.031225
25. A Ehyaie, M Hashemi, P Khadivi, in *World of Wireless, Mobile and Multimedia Networks and Workshops, WoWMoM, IEEE International Symposium*. Using relay network to increase life time in wireless body area sensor networks (IEEE, Kos, 2009), pp. 1–6
26. B Braem, B Latre, I Moerman, C Blondia, E Reusens, W Joseph, L Martens, P Demeester, in *Sensor Technologies and Applications, SensorComm, International Conference*. The need for cooperation and relaying in short-range high path loss sensor networks (IEEE, Valencia, 2007), pp. 566–571
27. B Chen, JP Varkey, D Pompili, J-J Li, I Marsic, in *Bioengineering Conference, Proceedings of the 2010 IEEE 36th Annual Northeast*. Patient vital signs monitoring using wireless body area networks (IEEE, New York, NY, 2010), pp. 1–2
28. X Sheng, J Tang, X Xiao, G Xue, Sensing as a service: challenges, solutions and future directions. Sensors J. IEEE. **13**(10), 3733–3741 (2013)
29. S-K Chen, T Kao, C-T Chan, C-N Huang, C-Y Chiang, C-Y Lai, T-H Tung, P-C Wang, A reliable transmission protocol for zigbee-based wireless patient monitoring. Inform. Technol. Biomed. IEEE Trans. **16**(1), 6–16 (2012)
30. T Watteyne, I AugÂt'e-Blum, M Dohler, D Barthel, in *Proceedings of the ICST 2nd international conference on Body area networks*. Anybody: a self-organization protocol for body area networks (ACM, Brussels, Belgium, 2007), p. 6
31. GR Tsouri, A Prieto, N Argade, On increasing network lifetime in body area networks using global routing with energy consumption balancing. Sensors. **12**(10), 13088–13108 (2012)
32. DH Chen, S Chan, J Bu, P Zhang, Secure and lightweight network admission and transmission protocol for body sensor networks. IEEE J. Biomed. Health Inform. (J-BHI). **17**(3), 664–674 (2011)
33. CA Otto, E Jovanov, A Milenkovic, in *Medical Devices and Biosensors*. A WBAN-based system for health monitoring at home (IEEE, Cambridge, MA, 2006), pp. 20–23
34. T Kuroda, H Sasaki, T Suenaga, Y Masuda, Y Yoshihiro, K Hori, N Ohboshi, T Takemura, K Chihara, H Yoshihara, Embedded ubiquitous services on hospital information systems. IEEE J. Biomed. Health Informatics (J-BHI). **16**(6), 1216–1223 (2012)
35. C Wang, Q Wang, S Shi, A distributed wireless body area network for medical supervision. Instrumentation and Measurement Technology Conference (I2MTC), 2012 IEEE International. (IEEE, Graz, 2012), pp. 2612–2616
36. M Zhang, A Sawchuk, Human daily activity recognition with sparse representation using wearable sensors. IEEE J. Biomed. Health Inform. (J-BHI). **17**(3), 553–560 (2013)
37. H Peng, F Long, C Ding, Feature selection based on mutual information criteria of max-dependency, max-relevance, and min-redundancy. Pattern Anal. Mach. Intell. IEEE Trans. **27**(8), 1226–1238 (2005)
38. S Ahmed, N Javaid, S Yousaf, A Ahmad, M Sandhu, M Imran, Z Khan, N Alrajeh, Co-laeeba: cooperative link aware and energy efficient protocol for wireless body area networks (2015). Computers in Human Behavior 51, Part B 1205–1215, computing for Human Learning, Behaviour and Collaboration in the Social and Mobile Networks Era doi:http://dx.doi.org/10.1016/j.chb.2014.12.051
39. S Hoceini, A Mellouk, A Chibani, Y Touati, B Augustin, Swarm intelligence routing approach in networked robots. Ann. Telecommunications-annales des tÂt'elÂt'ecommunications. **67**(7–8), 377–386 (2012)
40. S Akram, N Javaid, A Ahmad, Z Khan, M Imran, M Guizani, A Hayat, M Ilahi, A fatigue measuring protocol for wireless body area sensor networks. J. Med. Syst. **39**(12). doi:10.1007/s10916-015-0338-8. http://dx.doi.org/10.1007/s10916-015-0338-8
41. V Esteves, A Antonopoulos, E Kartsakli, M Puig-Vidal, P Miribel-Catal'a, C Verikoukis, Cooperative energy harvesting-adaptive MAC protocol for WBANs. Sensors. **15**(6), 12635–12650 (2015)